A SIMPLE DISTRIBUTED BACKPRESSURE-BASED SCHEDULING AND CONGESTION CONTROL SYSTEM

BY

ANTHONY J. HALLEY

B.S., Wright State University, 2005

THESIS

Submitted in partial fulfillment of the requirements
for the degree of Master of Science in Electrical and Computer Engineering
in the Graduate College of the
University of Illinois at Urbana-Champaign, 2007

Urbana, Illinois

Adviser:

Professor Nitin Vaidya

To Mom and Dad.

ACKNOWLEDGMENTS

First and foremost, I would like to acknowledge God for His continual blessings and guidance in my life. “And whatever you do, whether in word or deed, do it all in the name of the Lord Jesus, giving thanks to God the Father through him.” – Colossians 3:17.

I would also like to thank my adviser, Dr. Nitin Vaidya, for offering me a position in the Wireless Networking Group and guiding me through the thesis process. It has been an honor to work under him. I would also like to thank my many colleagues at the University of Illinois for their assistance during my time in the Wireless Networking Group. In no certain order, this includes Nistha Tripathi, Vijay Raman, Rishi Bhardwaj, Vartika Bhandari, Cheolgi Kim, Wonyong Yoon, Chandrakanth Chereddi, Pradeep Kyasanur, Matt Miller, Simone Merlin, Weihua Helen Xi, Dwayne Hagerman, and Michael Bloem.

TABLE OF CONTENTS

LIST OF TABLES

LIST OF FIGURES

CHAPTER 1

INTRODUCTION

1.1 Ad Hoc Networking and Cross-Layer Algorithms

It is difficult to walk down the street in the developed world and not spot some sort of wireless communication device in action. It could be any number of things: cell-phone, wireless-enabled laptop, Bluetooth headset, in-car GPS device, portable video game system, etc. Wireless connectivity has been changing from a consumer convenience to a consumer necessity. This trend is also apparent in other sectors such as military, corporate, medical, manufacturing, etc. With so many devices already out there and many more to come, it is desirable that these devices be able to communicate with one another, thus creating an ad hoc network. These devices will want to communicate with minimal delay and maximum throughput. It is the job of *most* ad hoc networking protocols to provide such a solution, and it is the goal of this thesis.

When searching for a solution for a good networking algorithm which has the aforementioned properties, it does not take long to discover the complexity involved. The classical approach is to break down the networking problem into smaller parts, called layers, and then optimize them individually. This modularization process serves its purpose well—to break down the problem into smaller, more-manageable pieces—however, all of this comes at the cost of overall optimization. By designing the layers exclusive of one another, the chances of the whole system being optimal are slim. Due to this sub optimality of the layered approach, we will focus on cross-layer networking solutions.

1.2 From Theory to Simulation

Many, if not all, electronic devices available on the market today are the *indirect* result of abstract theoretical works. The theories of which these products are the result are often based upon oversimplified models of the actual problem. However, that does not discredit the theory, but only makes the jump from theory to implementation tougher because the designer has to be able to (i) discover the stated and unstated simplifications and (ii) find ways to overcome them. In overcoming these simplifications, the designer has to make compromises that may hurt the theoretical performance while making the system more practical. In this thesis, we serve as the designers and try to find the delicate balance between practicality and performance.

The theoretical work, which we will discuss in more detail in Chapter 2, has proven that there exists a centralized scheduler which will provide maximal throughput. The scheduler uses the queue-length information of all nodes to schedule transmissions and transmission rates. In addition to providing maximal throughput, the scheduler guarantees the stability of the queues.

The congestion controller in [1], upon which our work is based, works to provide fairness for all flows by using the queue lengths to determine the flow rate at the application layer. The "cross-layer" term is due to the fact that the congestion controller is usually implemented at the transport layer and the queue length is found at the medium access (MAC) layer.

In this thesis, we take the scheduler and congestion controller and apply the theory to a decentralized protocol and simulate the protocol in the Network Simulator (NS2) [2].

1.3 Outline of Thesis

In Chapter 2, we provide the reader with some background materials, such as the 802.11 Distributed Coordination Function, and some related works in the areas of priority scheduling and backpressure-based scheduling. In Chapter 3, we summarize the system notation and the theoretical findings upon which this thesis is based. Then, in Chapter 4, we describe the design of a distributed backpressure-based scheduler and congestion controller. In Chapters 5 and 6 we discuss and analyze the performance of the distributed system, then summarize this thesis and suggest areas for future work.

CHAPTER 2

BACKGROUND AND RELATED WORK

2.1 802.11 Distributed Coordination Function (DCF) Medium Access Method

This work involves an adaptation of the 802.11 Distributed Coordination Function (DCF) medium access control (MAC) mode. The 802.11 standard describes two MAC modes: the DCF and Point Coordination Function (PCF) modes. The coordination functions control access to the wireless medium. The PCF mode is for infrastructure-based networks and is not discussed in this thesis (for further information on the PCF mode, refer to [3] or [4]). The DCF, on the other hand, is designed mainly for infrastructure-less networks and is what this thesis involves. The DCF mode allows many independent nodes to access the same wireless medium without the aid of a central entity. The mode uses a carrier sense multiple access (CSMA) scheme and collision avoidance (CA) to help access the medium while avoiding collisions. This type of system is referred to as CSMA/CA.

When trying to access the medium using the DCF mode, the node will always be performing carrier sensing. Carrier sensing is simply the act of sensing the channel to see if there is a transmission currently taking place or not. The carrier sensing will decide whether the channel is idle or busy. If carrier sensing finds the channel idle, then the node can contend for access to the channel. However, in DCF mode, a node cannot simply transmit whenever the channel is deemed idle; it must wait for a period of time referred to as the backoff window, or contention window.

Once a node gets a packet to send and wants to access the medium, it will first choose a value for its backoff interval, which we will refer to as b. This value is chosen randomly on the interval $[0, CW_{min}]$, where CW_{min} is a constant. We will refer to this interval as the contention window interval (CWI) and we will use the symbols CW_{lb} and CW_{ub} for the lower and upper bounds. The window corresponds to slots and a slot corresponds to a real time, which we will refer to as *slot_time*. So, once the node carrier senses the channel as idle, it will then start decrementing b every *slot_time* seconds. As long as the channel stays idle, the node will keep decrementing b until it gets to 0, and it will then send out its frame.[1] If there is no collision, then the receiving node will reply with an acknowledgment. Otherwise, the transmitting node will deem that a collision has taken place and exponentially increase its CWI upper bound, CW_{ub}, by multiplying it by two. The CWI upper bound is calculated according to

$$CW_{ub} = 2^{\log_2(CW_{min}+1)+i} - 1, \quad i \leq \log_2(CW_{max}+1) - \log_2(CW_{min}+1), \qquad (2.1)$$

where i is the number of consecutive collisions, $CW_{min} = \min(CW_{ub})$ and $CW_{max} = \max(CW_{ub})$. For example, if $CW_{min} = 31$ and $CW_{max} = 1023$, then $i \leq 5$ and as long as collisions happen, CW_{ub} will evolve as follows: 31, 63, 127, 255, 511, 1023.

Also, we should mention the interframe spacing (IFS). The two interframe spacings of interest are the DCF interframe space (DIFS) and the short interframe space (SIFS). The DIFS is the minimum idle time required before nodes can have immediate access to the medium. The SIFS is shorter than DIFS and is intended for use by high priority packets, such as positive acknowledgements.

We will wrap up our overview of the 802.11 DCF with a short example, shown in Figure 2.1. In this example, we have three nodes A, B, and C and let $CW_{min} = 7$. At t_0, both A and C get a packet from their upper layers to send to B. Nodes A and C then calculate backoff b over the interval $[0, 7]$, and they both happen to choose 4

[1] We assume that the RTS/CTS virtual carrier sensing method is not used here.

in this case. At t_1, all nodes sense the channel is idle. After waiting for the DIFS period, both A and C start counting down. At t_2, both A and C have counted down to 0, and they both transmit their data frames, which causes a collision. Since B could not receive either data frame due to the collision, no acknowledgement is sent. At t_3, both A and C have not received an acknowledgement and assume a collision has occurred. Using the new upper bound in (2.1), they recalculate their backoff b in the interval $[0, 15]$. We will assume A chooses 3 and C chooses 5. Once again, both A and C start to countdown. At t_4, A reaches 0 and retransmits its data frame. Node B then receives the data frame from A, waits for an SIFS period, and at t_5, sends an acknowledgement. After waiting for a DIFS period, node C restarts its countdown at t_6, and then after counting down to 0, sends its data frame to B, which is then acknowledged.

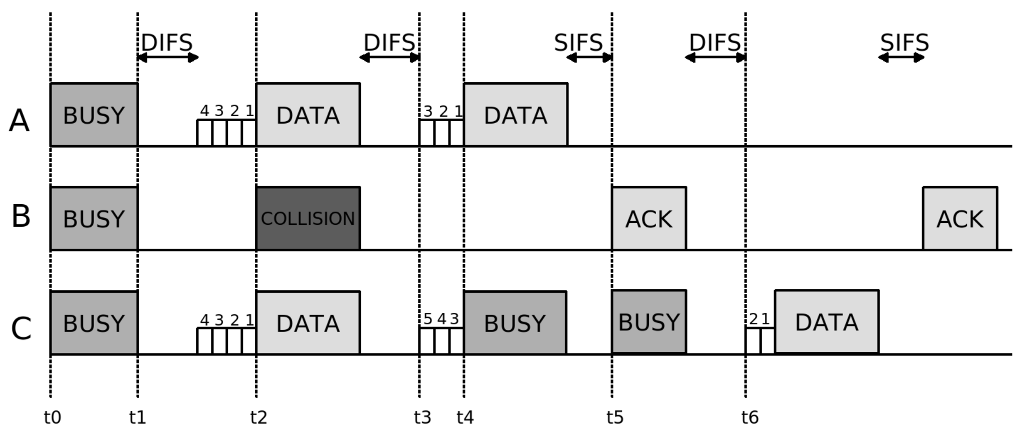

Figure 2.1: A simple example showing some properties of the 802.11 DCF MAC access mode. The small rectangles with the numbers above them represent backoff slots and are of duration *slot_time*.

2.2 802.11 Priority Schemes

In [5], the authors propose a priority scheme for the DCF access method of 802.11. They provide four priority levels. Two levels are created by changing the interframe spacing (IFS). In 802.11 DCF, once the channel has been declared idle by the carrier sensing mechanism, the node will wait for a DIFS period before starting to decrement its backoff counter. Deng and Chang [5] decided to create two DIFS period values, one for priority traffic, PIFS, and one for regular traffic, DIFS, where a PIFS period was shorter than a DIFS period. Thus, if two nodes had the same backoff value and sensed the channel as being idle at the same time, but one had a priority packet and the other did not, then the node with the priority packet would start counting down first and thus have a better chance of sending its priority packet before the regular packet. The second method of providing priority was via the backoff counter. In the regular 802.11 DCF, a packet would choose a random backoff value from the CWI $(0, CW_{ub})$, where CW_{ub} is calculated according to (2.1). To create prioritization, Deng et. al change the CWI to $(0, \frac{CW_{ub}}{2})$ for high priority packets and $(\frac{CW_{ub}}{2}, CW_{ub})$ for low priority packets. Thus, assuming no collisions, the high priority packets are guaranteed a lower backoff value b.

In [6], Xiao creates another priority scheme based upon the backoff mechanism. The author uses the following three metrics to differentiate the priority ith class: the initial window size $W_{i,0}$, the window-increasing factor σ_i, and the maximum backoff stage m_i, where σ_i is the factor by which the current window size is increased when a transmitted packet frame collides. In the 802.11 standard, the initial window size $(W_{i,0})$ is equal to 31, the window increasing factor (σ_i) is 2, and the maximum backoff stage (m_i) is 6. In this scheme, class i's backoff window is calculated by $\lfloor x \cdot \lceil (\sigma_i)^j W_{i,0} \rceil \rfloor$, where x is a uniform random variable in $(0, 1)$, j is the number of consecutive times a station tries to send a frame, $\lfloor y \rfloor$ represents the largest integer less than or equal to y, and $\lceil y \rceil$ represents the smallest integer greater than or equal to y. If priority class i has a higher priority than class j, then the authors declare $W_{i,0} \leq W_{j,0}$, $1 < \sigma_i \leq \sigma_j$, and $m_i \leq m_j$.

In [7], Vaidya et al. construct an algorithm to emulate Self-Clocked Fair Queuing (SCFQ) in a distributed manner. Given weights for each traffic flow, the goal is to have the throughput proportional to that weight. For example, if ϕ_i is the weight for flow i and T_i is the throughput for flow i, then the equality

$$\frac{T_i}{T_j} = \frac{\phi_i}{\phi_j}, \quad \forall i, j \tag{2.2}$$

should be maintained, assuming that both flows i and j are backlogged. As in the previous schemes, this also prioritizes traffic via an intelligent choice of the initial backoff interval, which reflects the weighting of the flow. However, this scheme, unlike [5] and [6] which simply prioritize traffic, attempts to achieve an *actual* ratio reflecting the weights of the flows, as seen in (2.2).

2.3 Queue-Length-Based Scheduling and Congestion Control

Tassiulas and Ephremides, in [8], were the first to address the issue of creating a stable scheduling algorithm for wireless networks. In that work, they consider all of the flow rates to be fixed, which we will refer to as *inelastic* traffic. Using the queue-length information at all of the nodes in the network, Tassiulas and Ephremides show that there is a scheduling algorithm which will stabilize those queues, assuming the arrival rates at the nodes are within the capacity region of the network. We will refer to any scheduler that can stabilize the queues for any set of flow rates that is within the capacity region as *throughput optimal*.

The idea introduced by Tassiulas and Ephremides was extended to incorporate *elastic* traffic via a distributed controller. This research was performed both in the wireline ([9], [10], [11], [12], [13], [14]) and wireless ([15], [16], [17], [18], [19], [20], [21], [22], [23], [24]) domains. These works prove that buffer stability, optimal routing, and fair rate allocation can be achieved using a distributed congestion controller and a queue-length-based scheduler. Although the congestion controller in the previous works was distributed, most of the schedulers used were centralized. A centralized scheduler is analyzed in [17], [20], [25], [26], [27], and [28]. We will use the cross-layer congestion control and scheduling framework developed in the works mentioned as a foundation for this thesis.

CHAPTER 3

SYSTEM MODEL AND THEORY

Most of this chapter is simply a summary of [1], but it is necessary to understand the future chapters and provides the underlying theory of the distributed algorithm. Most of the notation is the same as in [1].

3.1 System Model and Notation

In the model, we assume a network of nodes represented by the graph $\mathcal{G} = (\mathcal{N}, \mathcal{L})$, where $\mathcal{N}$ is the set of nodes and $\mathcal{L}$ is the set of directed links. If a link (n, m) is in $\mathcal{L}$, then it is possible to send packets from node n to node m subject to the interference constraints. The link rate vector is represented by $\mu = \{\mu_l\}_{l \in \mathcal{L}}$, where μ_l is the rate at which data can be transferred over link l. Each link rate, μ_l, has an upper bound, given by $\hat{\eta} < \infty$.

We let $\hat{\Gamma}$ denote the bounded region in the $|\mathcal{L}|$-dimensional real space, representing the set of μ that can be achieved in a given time slot. This can also be described as the interference constraint. This set, in general, need not be convex. Typically, $\hat{\Gamma}$ would be a discrete set of rates that can be achieved, and thus would be nonconvex. So, in order to obtain a convex set, we take the convex hull and denote it by $\Gamma = \mathcal{CH}\{\hat{\Gamma}\}$. Any point in Γ can be achieved by time-sharing between rate vectors in $\hat{\Gamma}$.

The set of all flows that are sharing the network resources is denoted by $\mathcal{F}$. The beginning and ending nodes for the flow f are given by $b(f)$ and $e(f)$. A sample network with flows can be seen in Figure 3.1(a).

Every flow f has a utility function $U_f(x_f)$ associated with it, which is a function of

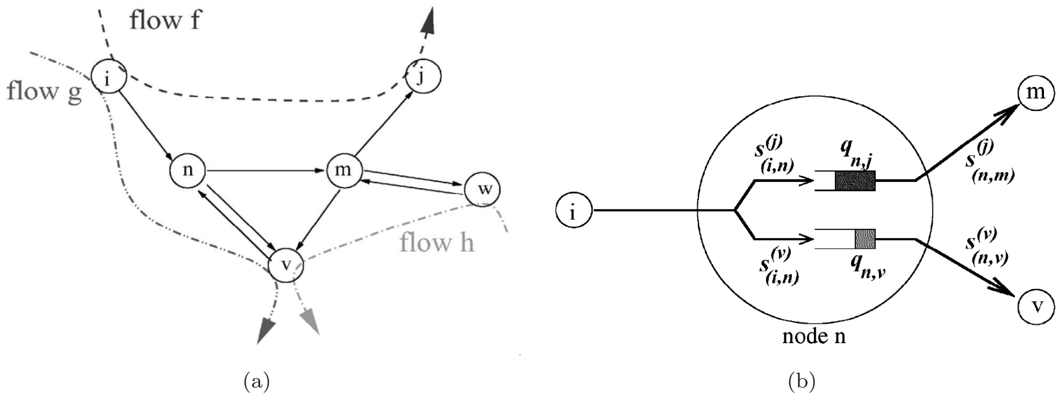

Figure 3.1: An example network showing flows and the queues per destination. In (a), we see an example network model with $b(f) = i$, $e(f) = j$, $b(g) = i$, $e(g) = v$, and $b(h) = w$, $e(h) = v$. Every node contains a queue for each destination node. Figure (b) zooms into node n of figure (a). Source: [1].

the flow rate x_f. The utility function is assumed to satisfy the following conditions:

- $U_f(\cdot)$ is a twice differentiable, strictly concave, nondecreasing function of the flow rate x_f.
- For every m and M satisfying $0 < m < M < \infty$, there exist constants $\tilde{c}$ and $\tilde{C}$ satisfying $0 < \tilde{c} < \tilde{C} < \infty$ such that

$$\tilde{c} \leq -\frac{1}{U_f''(x)} \leq \tilde{C}, \qquad \forall x \in [m, M]. \tag{3.1}$$

These conditions are met by the following class of utility functions:

$$U_f(x) = \beta_f \frac{x^{1-\alpha_f}}{(1-\alpha_f)}, \qquad \forall \alpha_f > 0. \tag{3.2}$$

This class of utility functions has been shown to characterize a large class of fairness concepts [29]. In this thesis, however, we will focus on utility functions of the form

$$U_f(x) = \beta_f \ln(x), \tag{3.3}$$

where $U_f'(x) = \frac{\beta_f}{x}$, $U_f''(x) = -\frac{\beta_f}{x^2}$, and $\beta_f > 0$.

We will now describe the capacity region of the network.

Definition 1 (Capacity Region)**.** The capacity region Λ of the network contains the set of flow rates $\{x_f\}_{f\in\mathcal{F}} \geq \mathbf{0}$ for which there exists a set $\left\{\mu_l^{(d)}\right\}_{l\in\mathcal{L}}^{d\in\mathcal{N}}$ that satisfies

- $\left[\sum_d \mu_l^{(d)}\right] \in \Gamma$, where $\mu_l^{(d)} \geq 0$ for all $l \in \mathcal{L}$, $d \in \mathcal{N}$.
- $\mu_{into(n)}^{(d)} + \sum_f x_f \mathcal{I}_{\{b(f)=n,e(f)=d\}} \leq \mu_{out(n)}^{(d)}$ for each $n \in \mathcal{N}$, and $d \neq n$, where $\mu_{into(n)}^{(d)} := \sum_{(k,n)\in\mathcal{L}} \mu_{(k,n)}^{(d)}$ and $\mu_{out(n)}^{(d)} := \sum_{(n,m)\in\mathcal{L}} \mu_{(n,m)}^{(d)}$. Notice that $\mu_{into(n)}^{(d)}$ (or $\mu_{out(n)}^{(d)}$) denotes the *potential* number of packets that are destined for node d, incoming to (or outgoing from) node n. Here, $\mathcal{I}_{a=b}$ is the identity function, where $\mathcal{I}_{a=b} = 1$ if $a = b$ and $\mathcal{I}_{a=b} = 0$ if $a \neq b$.

At every node, there is a queue for each flow having the same destination. We will use $q_{n,d}[t]$ to denote the number of packets that are destined for node d, waiting for service at node n at time t. Figure 3.1(b) shows an example of such queues. The evolution of the queues is then given by

$$q_{n,d}[t+1] = q_{n,d} + \sum_f x_f[t]\mathcal{I}_{\{b(f)=n,e(f)=d\}} + s_{into(n)}^{(d)} - s_{out(n)}^{(d)}[t], \qquad \forall n \in \mathcal{N}, d \in \mathcal{N}\setminus\{n\}, \tag{3.4}$$

where $s_{into(n)}^{(d)} := \sum_{(k,n)\in\mathcal{L}} s_{(k,n)}^{(d)}$ and $s_{out(n)}^{(d)}[t] := \sum_{(n,m)\in\mathcal{L}} s_{(n,m)}^{(d)}$, and $s_{(n,m)}^{(d)}$ denotes the rate provided to d-destined packets over link (n,m) at slot t (a slot is 1 unit time). It is important to note the distinction between s and μ: $s_{(n,m)}^{(d)}[t]$ denotes the *actual* amount of packets served over the link, whereas $\mu_{(n,m)}^{(d)}[t]$ denotes the *potential* amount served. Thus, $s_{(n,m)}^{(d)}[t] = \min(\mu_{(n,m)}^{(d)}[t], q_{n,d}[t])$ for all $(n,m) \in \mathcal{L}$, $d \neq n$. We also let $s_{(n,m)}[t] = \sum_d s_{(n,m}^d[t]$, which is the total amount of traffic served over link (n,m). We will refer to the queues with destinations, $q_{n,d}$, as queue's-per-destination, or QPDs. Also, the sum of all QPDs at a given node will be called the overall queue, or OQ.

3.2 Problem Statement and Optimal Point

The goal of Eryilmaz et al. in [1] was to design a congestion control, scheduling mechanism such that the flow rate vector $\mathbf{x}$ solves the following optimization problem:

$$\max_{\mathbf{x}\in\Lambda} \sum_{f\in\mathcal{F}} U_f(x_f). \tag{3.5}$$

Due to the strict concavity assumption of $U_f(\cdot)$ and the convexity of the capacity region Λ, there does exist a unique optimizer to (3.5), which we will further refer to as $\mathbf{x}^\star$, or the *fair rate allocation* point. We will also refer to an element out of $\mathbf{x}^\star$ as $x_f^\star$.

3.3 Backpressure-Based Centralized Scheduling Algorithm

Introduced by Tassiulas and Ephremides [8], the centralized scheduling algorithm upon which our work is based is known as the *back-pressure scheduler*. This scheduler uses the differential backlog at the two end-nodes of a link to determine the rate of that link. The idea behind the scheduler can be explained simply. Assume we have a flow f which must take a route consisting of three nodes: $(n_a \to n_b \to n_c)$. The idea behind the backpressure based scheduler is to schedule traffic such that, in this case, the middle node n_b does not get overloaded with packets from n_a, but will have a similar link rate from $n_b \to n_c$ as the link $n_a \to n_b$. By doing so, the queues at n_a and n_b will be stable and the traffic over the links will also be stable.

Definition 2 (Back-pressure Scheduler)**.** At slot t, for each $(n,m)\in\mathcal{L}$, we define the differential backlog for destination node d as $W_{(n,m),d}[t] := (q_{n,d}[t] - q_{m,d}[t])$. Also, we let $W_{(n,m)}[t] = \max_d \left\{W_{(n,m),d}[t]\right\}$ and $d_{(n,m)}[t] = \arg\max_d \left\{W_{(n,m),d}\right\}$. Then, choose the rate vector $\mu[t] \in \mathcal{L}$ that satisfies

$$\mu[t] \in \arg\max_{\{\eta \in \Gamma\}} \sum_{\{(n,m) \in \mathcal{L}\}} \eta_{(n,m)} W_{(n,m)}[t], \tag{3.6}$$

then serve the queue holding packets destined for node $d_{(n,m)}[t]$ over link (n, m) at rate $\mu_{(n,m)}[t]$. Effectively, this is setting $\mu_{(n,m)}^{(d_{(n,m)}[t])}[t] = \mu_{(n,m)}[t]$. The rest of the queues at node n are not served at slot t.

3.4 Congestion Controller

Definition 3 (Congestion Controller)**.** At the beginning of time slot t, each flow, say f, has access to the queue length of its first node, $q_{b(f),e(f)}[t]$. The data rate $x_f[t]$ of flow satisfies

$$x_f\,[t+1] = \left\{ x_f[t] + \alpha(KU'(x_f[t]) - q_{b(f),e(f)}[t]) \right\}_m^M, \tag{3.7}$$

where the notation y_a^b projects the value of y to the closest point in the interval $[a, b]$. We assume that m is a fixed positive valued quantity that can be arbitrarily small, $M > 2\hat{\eta}$, and $K > 0$.

In [1], the authors prove the following theorem, which shows that the average rate obtained for each flow can be made arbitrarily close to its fair share, according to (3.5), by choosing a sufficiently large K.

Theorem 1. For $\alpha = (1/K)^2$, and for some finite $B > 0$, we have: for all $f \in \mathcal{F}$

$$x_f^\star - \frac{B}{\sqrt{K}} \leq \liminf_{T \to \inf} \frac{1}{T} \sum_{t=0}^{T-1} x_f[t] \leq \limsup_{T \to \inf} \frac{1}{T} \sum_{t=0}^{T-1} x_f[t] \leq x_f^\star + \frac{B}{\sqrt{K}}. \tag{3.8}$$

CHAPTER 4

DESIGN OF DISTRIBUTED CONTROLLER AND SCHEDULER

In this chapter, we will first discuss our simulation tool and then discuss the design and implementation of the scheduler and congestion controller.

4.1 NS2 and MIRACLE

The Network Simulator [2], which we will further refer to as NS2, is an open source discrete event simulator aimed at networking research. NS2 is comprised of two parts: an object oriented simulator, written in C++, and an interpreter, written in object oriented Tool Command Language (OTcl). The simulator portion is built for speed and allows simulations with tens to hundreds of nodes with hundreds of flows to take less than real time. The interpreter, on the other hand, is meant for the user to be able to have access to all aspects of the scenario (network topology, traffic generation, protocol parameters) without having to change and recompile the C++ code.

While NS2 was originally created for wireline networks, it has since been extended for wireless networks. The original wireless extensions for NS2 were authored by CMU's Monarch group. A schematic of a mobile node under the CMU Monarch's wireless extensions is given in Figure 4.1. While we will not go into detail about every aspect of the mobile node,[1] it is important to note the functionality of some of the blocks:

- Link layer (LL): If the packet is outgoing, the LL module's main job is to set the MAC destination address in the MAC header of the packet. To achieve this,

[1] The reader can find more detailed information in [30].

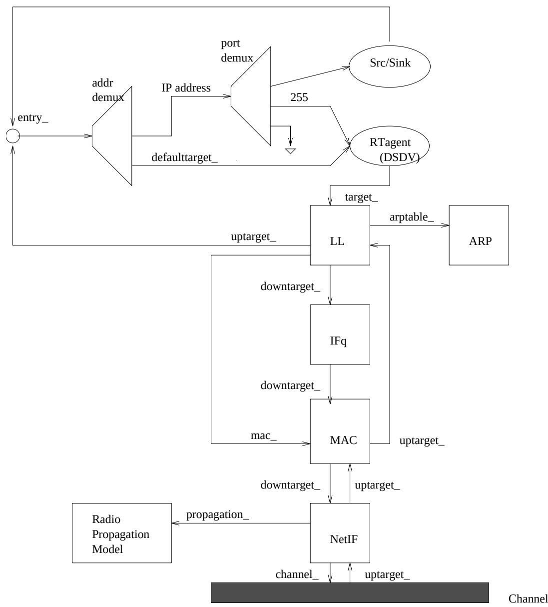

Figure 4.1: Schematic of a mobile node under the CMU Monarch's wireless extensions. Source: [2].

there is an ARP module connected to it which will perform the Internet protocol (IP) destination address to MAC hardware address conversion. Once the MAC address has been placed in the header, the packet is passed down to the IFq.

- Address resolution protocol (ARP): The ARP module receives requests from the LL wanting MAC addresses resolved from IP addresses. If the ARP module already has a MAC address for the corresponding IP address, then it immediately responds with that MAC address. If not, it immediately broadcasts an ARP query and caches the packet temporarily.

- Interface queue (IFq): The IFq is a simple queue module with priority for control packets. If the IFq receives a control packet such as a routing protocol packet, it will immediately put it at the head of the queue. Some aspects of this module will later be modified to implement the scheduler.

- Medium access control (MAC): The 802.11 DCF MAC has been implemented in this module by the CMU Monarch team. It implements both virtual and physical carrier sensing and uses the RTS/CTS/DATA/ACK pattern for unicast packets and just DATA for broadcast packets. Some aspects of this module will later be modified to implement the scheduler.

In order to keep a strict modularized network stack, most layers in NS2 are only designed to send packets up or down with no other communication between layers taking place. In the system in this work, cross-layer communication is important and necessary for easy implementation. Thus, the Multi-Interface Cross-Layer Extension library for the Network Simulator (NS-MIRACLE) [31] was used.

NS-MIRACLE is a set of libraries which extend NS2 and allow for easy exchange of messages from one layer to another (cross-layer messages). NS-MIRACLE also allows for placing multiple modules at each layer (e.g., multiple physical layer modules to simulate a node with multiple network interfaces). An example node showing the core components of the NS-MIRACLE extension can be seen in Figure 4.2. The modules

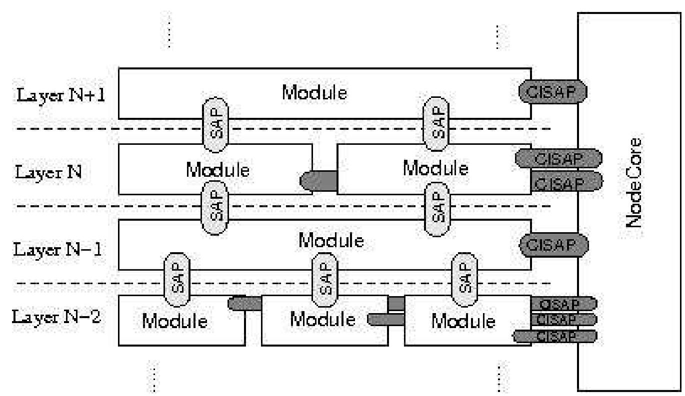

Figure 4.2: An example node using the NS-MIRACLE extension to NS2. Source: [31].

make up the layers of the network stack and are designed to contain the corresponding layer's protocol. The communication between modules in adjacent layers is performed through a channel known as a service access point (SAP). These two components, modules and SAPs, allow the node to operate in a layered sense and conform to the Open System Interconnection (OSI) reference model. However, NS-MIRACLE also adds cross-layer messaging capabilities through the NodeCore and cross-layer SAP (ClSAP) channels. All modules are equipped with a ClSAP that is connected to the NodeCore. The NodeCore serves as a cross-layer bus that will carry cross-layer messages from any module to any other module. The cross-layer messages are also fully customizable to allow the designer maximum flexibility.

The node structure used in this work can be seen in Figure 4.3. We will briefly

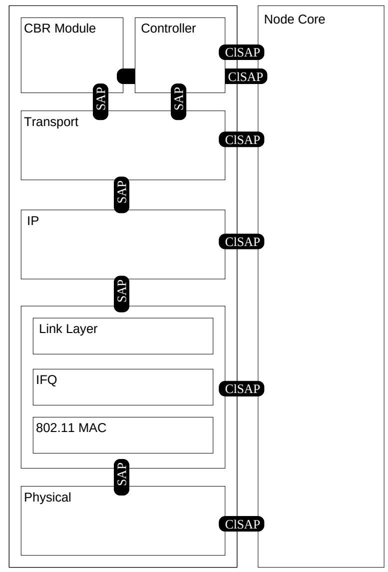

Figure 4.3: An example of the node structure used in this work.

explain the functionality of each module:

- CBR Module: The constant bit rate (CBR) module is used to introduce traffic into the system. The module delivers packets to the layer below at a constant rate, which we will commonly refer to as the flow rate, or arrival rate (with respect to the queue). The congestion controller will serve to control the flow rate.

- Controller: This module contains the core of our work. We will elaborate more on this module later, but basically, it generates the backpressure-information broadcast packets, performs the congestion control calculations, and performs the distributed scheduling.

- Transport: This module currently just passes packets along. If it is an outgoing packet, then it passes it down to the lower layer and vice versa for an incoming packet. This module is only placed here to allow for later expansion.

- IP: The IP module performs the routing. The packets generated from the CBR module have a destination address and the IP module converts that address to a next-hop address. Once the next-hop address has been placed in the packet header, the packet is sent on to the lower layer. If the packet is an incoming packet, the IP layer first figures out if this node is the final destination or not. If so, the packet is passed on to the upper layer. If not, the node needs to forward this packet on, so the next-hop address is placed into the header and the packet is then sent on to the lower layer.

- MAC: This module contains three NS2 components, the Link Layer (LL), the interface queue (IFQ), and the 802.11 MAC. These are the same components shown in Figure 4.1 and explained above.

- Physical (PHY): The Physical (PHY) module performs some simple signal to interference plus noise (SINR) threshold testing to decide whether or not packets have been correctly received.

4.2 Distributed Congestion Controller

The congestion controller is discussed in Section 3.4 and updates the flow rate iteratively based upon the current queue length at the source node and the derivative of the utility of the flow. In order to avoid large oscillations of the flow rate, we will use a modified version of (3.7), given by

$$x_f\left[t+\Delta_{cc}\right] = \left\{x_f[t] + \alpha(KU'(x_f[t]) - q_{b(f),e(f)}[t])\right\}_{m'}^{M'}, \tag{4.1}$$

where $m' = \max\{m, \frac{x_f[t]}{2}\}$, $M' = \min\{M, 2x_f[t]\}$, m and M are constant scalars, and Δ_{cc} is the time between rate updates. In most of our simulations, $m = 1$ pkts/sec and $M = 200$ pkts/sec. The m' and M' serve to put hard limits on the rate of change and their need will be shown in the next section. Similar ideas are implemented in versions of the transport control protocol (TCP).

In our NS2 model, we place the congestion controller in the Controller module, as shown in Figure 4.3. Every Δ_{cc} seconds, the Controller sends a cross-layer message (ClMessage) to the MAC module, requesting the current queue length. When the MAC module receives that query, it immediately responds with another ClMessage which contains the current queue length for the flow, or flows, being generated by this node. Once the Controller receives the ClMessage containing the queue length, it updates the rate according to (4.1) and then sends a ClMessage to the CBR module which contains the updated rate. On receipt of the rate update ClMessage, the CBR module will then update its timer to accurately reflect the new flow rate.

The CBR module generates packets every Δ_{CBR} s, where $\Delta_{CBR} = \frac{\text{packetSize}}{x_f}$. The module uses a timer to schedule packet generation. When the timer expires, a packet is sent to the layer below. When a rate update cross-layer message is received from the Controller, the CBR timer is updated according to

$$T_{np} = \max\left(\Delta_{new} - (t_c - t_{lp}), 0\right), \tag{4.2}$$

where T_{np} is the time until the next packet generation, Δ_{new} is the new packet interval, t_c is the current time, and t_{lp} is the time the last packet was generated. So, after this update, the next packet will be scheduled to be generated in T_{np} s, or at simulation time $t_c + T_{np}$.

4.2.1 Optimal flow rate

Later in our simulations, it will be valuable to know what the optimal fair rate allocation is for certain scenarios. Let us start with a simple scenario with four flows and calculate the optimal flow rates using Lagrange multipliers. Let $f(x_1, x_2, x_3, x_4)$ be the function which we are trying to optimize and let $g(x_1, x_2, x_3, x_4)$ be the constraint. Recall that our optimization problem is $\max_{\mathbf{x}} \sum_f U(x_f)$, where x_f is the flow rate of flow f. Function $f(\cdot)$ is given by

$$f(x_1, x_2, x_3, x_4) = \beta_1 ln(x_1) + \beta_2 ln(x_2) + \beta_3 ln(x_3) + \beta_4 ln(x_4), \tag{4.3}$$

where β_1-β_4 are constants. We also have the following constraint:

$$g(x_1, x_2, x_3, x_4) = x_1 + x_2 + x_3 + x_4 \leq C, \tag{4.4}$$

where C represents the maximum achievable throughput. Setting $\nabla f = \lambda g$ and including the constraint, we are left with the following five equations:

$$\frac{\beta_1}{x_1} = \lambda \tag{4.5}$$

$$\frac{\beta_2}{x_2} = \lambda \tag{4.6}$$

$$\frac{\beta_3}{x_3} = \lambda \tag{4.7}$$

$$\frac{\beta_4}{x_4} = \lambda \tag{4.8}$$

$$x_1 + x_2 + x_3 + x_4 = C. \tag{4.9}$$

Using simple algebraic manipulation, we see that the optimal flow rates are given by

$$x_k^\star = \beta_k \left(\frac{C}{\beta_1 + \beta_2 + \beta_3 + \beta_4} \right), \quad \forall k \in 1, 2, 3, 4. \tag{4.10}$$

For a simple example, let $C = 1$ Mbps and $\beta = [1, 2, 3, 4]$; then the optimal flow rates are $\mathbf{x}^\star = [100, 200, 300, 400]$ kbps. Note that the sum of the flow rates equal 1 Mbps, as expected. This can be generalized to any amount of flows,

$$x_k^\star = \beta_k \left(\frac{C}{\sum_{f \in \mathcal{F}} \beta_f} \right), \quad \forall k \in \mathcal{F}, \tag{4.11}$$

and the optimal value of the summation can be given by

$$\sum_{f} U(x_f^\star) = \sum_{k\in\mathcal{F}} \beta_k \ln\left(\beta_k\left(\frac{C}{\sum_{f\in\mathcal{F}}\beta_f}\right)\right). \tag{4.12}$$

4.3 Distributed Backpressure-Based Scheduler

The goal of the backpressure scheduler is to normalize the queues in the network. The centralized scheduler in Section 3.3 uses the differential backlog at the end nodes of a link, i.e., the backpressure, to determine the rate of that link. Effectively, it provides a high rate to those nodes with the highest backpressure in the network. By assigning a higher rate to those nodes with a high backpressure, the scheduler is attempting to decrease the backpressure at those nodes and, in turn, normalize the queues of the network.

The centralized scheduler is proven to work, but we are interested in a scheduler that is distributed and does not need information about every node in the network. In order to do so, the following two main questions must be answered:

- How is the backpressure information going to be obtained?
- Once the backpressure has been obtained, how is the node going to use that information?

For the first item, each node will periodically send out a broadcast packet containing its own queue information, as well as its backpressure information. The recipient of this broadcast packet can then (i) calculate its own backpressure using the queue length of the sending node, and (ii) compare backpressure values with the neighboring node. The format of an example broadcast packet can be seen in Table 4.1. According to the example packet, at node n, $q_{n,m_1} = 5$, $q_{n,m_2} = 40$, $q_{n,m_3} = 10$, $W_{n,m_1} = 2$, $W_{n,m_2} = 25$, and $W_{n,m_3} = 0$, where $W_{n,d} = (q_{n,d} - q_{x,d})$ with x representing the next hop for packets destined for d.

Table 4.1: Sample broadcast packet from node n which has packets destined for m_1, m_2, and m_3.

Destination (2 bytes)	Queue Length (2 bytes)	Backpressure (2 bytes)
m_1	5	2
m_2	40	25
m_3	10	0

Upon arrival of that broadcast packet from n, the receiving node, say r, does two things. First, r checks to see if n is the next hop for any of the destinations for which it has queues. If so, r then calculates the backlog. So, continuing with the example, if there is a flow with route r-n-$(\cdots)$-m_2, then when r receives the broadcast packet, it will update its backpressure to $W_{(r,n),m_2} = q_{r,m_2} - q_{n,m_2} = q_{r,m_2} - 40$. Secondly, r will take the maximum backpressure from the packet, $\max_d W_{n,d}$, and update its neighbor backpressure table (NBT). The NBT is simply a table containing the neighbor's ID and its maximum backpressure. A neighbor is added any time a broadcast is received from that node. A sample for r can be seen in Table 4.2.

Table 4.2: A sample neighbor backpressure table (NBT) for node r.

Neighbor (N)	Backpressure (W)
n	22
N_2	32
N_3	13
N_4	0

Assuming that r has the backpressure values for all of r's neighbors, r now has to decide how to use those backpressure values. This brings us to the second item, that is, how to use the local backpressure values. In the centralized scheme, link rates are chosen according to (3.6), a maximization of a weighted sum. This maximization would most likely result in the links with high backpressure getting high link rates alloted to them and vice versa with links with low backpressure.

Using this basic concept, we developed a distributed scheduler on top of the 802.11 MAC. As explained in Section 2.1, the 802.11 DCF chooses a random backoff value when it has a packet to transmit. This backoff value was created to deal with contention in the network. Depending on the level of contention in the network, the backoff value may be either large (high contention) or small (low contention). In addition, a node with a small backoff value will have faster access to the channel than a node with a large backoff value. It is simple to see that this value can be used as a priority mechanism for channel access. For example, if a node has high (low) priority traffic then it can set its backoff value low (high). By doing so, it is more likely that the high priority traffic will obtain a higher throughput. Some prior 802.11 priority schemes are mentioned in Section 2.2.

The goal of our scheduler is to allow nodes with high backpressure to transmit more often than nodes with low backpressure. To do so, we will take advantage of 802.11 DCF backoff value and treat the backpressure as a priority value, where a high backpressure represents high priority traffic.

As explained in Section 2.1, the backoff value (b) is chosen uniformly on the interval $[CW_{lb}, CW_{ub}]$, where $CW_{lb} = 0$ in the 802.11 standard, and CW_{ub} evolves according to (2.1). With the goal of prioritizing based on backpressure, we have created the following two schemes for our scheduler:

1. This scheme simply changes CW_{min} based upon the backpressure values of the node in question, n, and its neighbors, $nbr(n)$. The node first calculates the minimum and maximum backpressure values among itself and its neighbors:

$$W_{max} = \max_{\substack{(k,m) \\ k \in \{nbr(n), n\}}} \{W_{(k,m)}\}$$

$$W_{min} = \min_{\substack{(k,m) \\ k \in \{nbr(n), n\}}} \{W_{(k,m)}\}.$$

   Then, it sets its contention window minimum value according to

$$CW_{min} = (CW_{umax} - CW_{umin}) \left(1 - \frac{W - W_{min}}{W_{max} - W_{min}}\right) + CW_{umin}, \qquad (4.13)$$

   where CW_{umin} and CW_{umax} are user-supplied values that set the minimum and maximum CW_{ub}, $CW_{umax} \geq CW_{umin}$, and $W = \max_m W_{(n,m)}$. Basically, this is a simple linear mapping function that maps high backpressure to low contention window values. For example, if $W = W_{max}$, then $CW_{min} = CW_{umin}$ and the node will pick a b along the interval $[0, CW_{umin}]$. Likewise, if $W = W_{min}$, then the node will pick a b along the interval $[0, CW_{umax}]$. In this scheme, $CW_{lb} = 0$ always and CW_{ub} evolves according to (2.1), but with CW_{min} changing.

2. This scheme is loosely based on [5] and changes both CW_{ub} and CW_{lb}. In scheme 1, there is a nonzero probability that a node with $CW_{min} = 255$, for example, could gain access to the channel before a node with $CW_{min} = 31$ because b is chosen over the interval $[0, CW_{ub}]$. We will use a similar mapping as the other schemes, but use the value calculated as a mean value. That is,

$$CW_{avg} = (CW_{umax} - CW_{umin}) \left(1 - \frac{W - W_{min}}{W_{max} - W_{min}}\right) + CW_{umin} \tag{4.14}$$

and

$$CW_{lb} = \max \{CW_{avg} - \sigma, 0\} \tag{4.15}$$

$$CW_{ub} = CW_{avg} + \sigma. \tag{4.16}$$

As an example case, let us assume that $W_{max} = 200$, $W_{min} = 50$, and $W = 75$. Also, let $CW_{umax} = 511$ and $CW_{umin} = 31$. This would result in $CW_{avg} = 431$. Further, letting $\sigma = 10$, we have $CW_{lb} = 421$ and $CW_{ub} = 441$. So, in this scheme, b would be chosen randomly from the interval [421,441], whereas in scheme 1 it would be chosen from [0,431].

CHAPTER 5

SIMULATIONS AND ANALYSIS OF DISTRIBUTED ALGORITHM

5.1 Scenarios

Before we go through the simulations we have performed, we will first clearly explain the general scenario layouts for our simulations. When these scenarios are referred to later, assume that everything is exactly the same as explained here, *unless* it is specifically stated otherwise. All the scenarios can be seen in Figure 5.1.

1. **Symmetric local area network**: This is a simple layout with 8 or 16 nodes spread out equidistant along the edge of a circle. The diameter of the circle is 175 m, whereas the transmission range is 250 m, so all nodes are within transmission range of each other. To see the layout of the nodes refer to Figures 5.1(a) and 5.1(b). This scenario is used to see how the scheduler and controller perform in a one-hop environment.

2. **Multihop multiflow straight line**: This layout involves nodes in a straight line with multiple hop flows. All of the flows have the same forwarding nodes, thus making the forwarding nodes make use of their per-destination queues. This scenario was used to analyze the ability of the scheduler to handle forwarding multiple flows to different destinations.

3. **Multihop random**: The random scenarios consist of eight 3-hop disjoint (i.e., no flow shares the same forwarding nodes) flows placed randomly in a 1000 m x 1000 m scenario. The scenarios were generated by first placing 100 nodes randomly in the square scenario (Figure 5.1(e)) and then using Dijsktra's shortest

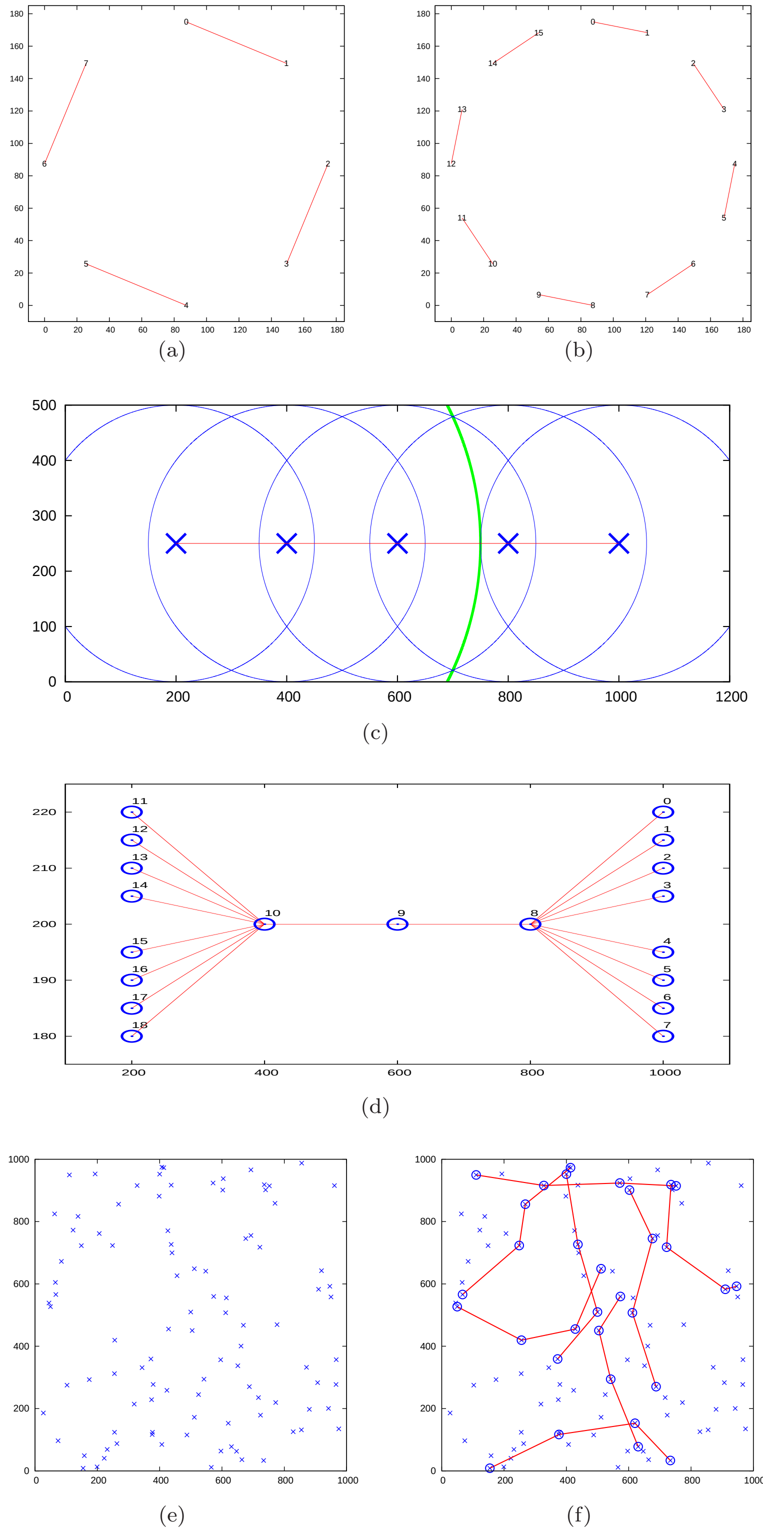

Figure 5.1: Scenario layouts. Both the x- and y-axes are distance in meters. In (c), the smaller radius circles show the transmission range and the broad line at $x \approx 700$ m shows the carrier sense of the leftmost node. In (d) and (e), notice that the figure is not to scale.

hop algorithm to find eight 3-hop disjoint flows (Figure 5.1(f)). This scenario was chosen to analyze the robustness of the scheduler and controller.

5.1.1 NS2 parameters

Like most network simulation tools, there are many input parameters and NS2 is not unlike the others. In Table 5.1, we have placed all the uniform parameters across all scenarios. If we deviate from these values, it will be clearly stated. In order to

Table 5.1: NS2 scenario properties.

Property	Value	Unit
Data Rate	1	Mbps
Basic Rate	1	Mbps
Propagation Model	Two Ray Ground	-
Transmit Power (P_t)	24.5	dBm
CS Threshold	-78	dBm
CP Threshold	10	dBm
RX Threshold	-64	dBm
CS Range	550	m
TX Range	250	m
Initial Rate ($x_f[0]$)	50	pkts/sec
Packet Size	1,000	bytes
Maximum Queue Size	10,000	pkts
Minimum Rate (m)	1	pkt/sec
Maximum Rate (M)	200	pkts/sec
RX Antenna Gain (G_r)	1	-
TX Antenna Gain (G_t)	1	-
RX Antenna Height (h_r)	1.5	m
TX Antenna Height (h_t)	1.5	m

understand what all of these values mean, we will briefly explain each:

- Data rate: The bit rate at which DATA packets can be transmitted.
- Basic rate: The bit rate at which control/management packets are transmitted.
- Propagation model: The model used to calculate the propagation of the wireless signal. Here we have used the two-ray ground propagation model, which is defined in [32] as

$$P_r = P_t G_t G_r \frac{h_t^2 h_r^2}{d^4}, \quad \text{for } d \gg \sqrt{h_t h_r} \tag{5.1}$$

where P_r and P_t are the received and transmitted power, G_r and G_t are the receiver and transmitter antenna gain constants, h_r and h_t are the height of the receiver and transmitter antenna, and d is the distance between the transmitter and receiver.

- CS threshold: If the received power is below the carrier sense (CS) threshold, then the channel is deemed to be idle.

- CP threshold: Suppose a packet A arrives at node n with receive power $P_r(A)$ at $t = 0$ and is not done being received until $t = 1$. Now also assume that another node transmits a packet B and it arrives at n at $t = 0.5$ with power $P_r(B)$. Now, NS2 compares the received powers to decide whether packet A will be correctly received. The decision is made according to

$$10 \log(P_r(A)) - 10 \log(P_r(B)) \underset{\text{collision}}{\overset{\text{no collision}}{\gtrless}} CP_{thresh}, \tag{5.2}$$

where CP_{thresh} is the capture threshold in dBm.

- RX threshold: The receive threshold is the receive power threshold below which a packet cannot be correctly decoded, or received.

- CS range: Given the transmit power and the carrier sense threshold, this is the range at which a node can sense another node transmitting a packet.

- TX range: Given the transmit power and the receive threshold, and assuming no interference, this is the range at which a node can correctly decode a packet.

- Initial rate: The initial CBR flow rate at the beginning of the simulation (at $t = 0$).

- Packet size: The size of the DATA packets generated by the CBR module.

- Maximum queue size: The maximum size of the queue. If the queue overflows, packets will be discarded.

- Minimum rate: The minimum flow rate of the congestion controller.
- Maximum rate: The maximum flow rate of the congestion controller.

5.2 Simulations

5.2.1 Symmetric local area network

In these scenarios, all nodes are within the transmission range of all other nodes. Thus, only one node can transmit at a time without causing a collision. The 4-flow and 8-flow scenario can be seen in Figure 5.1.

In this set of simulations, we want to see the following two things:

- The effect of changing the frequency of the backpressure broadcasts. We will denote the backpressure broadcast frequency as

$$BP_{freq} = \frac{1}{\Delta_{bp}}, \tag{5.3}$$

  where Δ_{bp} denotes the time, in seconds, between each broadcast of backpressure information.

- The effect of using the two different congestion window update schemes in the distributed scheduler, as explained in Section 4.3.

We would expect to see a unique optimal value of BP_{freq}, considering that too few broadcasts would hurt the performance of the scheduler, but too many broadcast packets will hurt overall throughput.

To gauge performance, we will look at the following metrics:

- Simulation average throughput: The CBR throughput averaged over the entire simulation. In particular, we will compare this performance against the regular 802.11 throughput with each node always being backlogged. This will give us an idea of the efficiency of the scheduler and the impact of the broadcast packets.

The simulation average throughput is calculated as

$$TP_{avg}(0,T) = \frac{1}{T} \sum_{f \in \mathcal{F}} r^{f}_{e(f)}(0,T), \tag{5.4}$$

where T is the simulation time in seconds and $r^f_n(t_1, t_2)$ represents the number of packets from flow f received by node n in the interval $[t_1, t_2]$.

- Average sum of utility: The goal of this system is to optimize the sum of the utilities according to (3.5). This metric is calculated as

$$U^{avg}_{sum}(T_{stable}, T) = \frac{1}{|\mathcal{T}|} \sum_{t \in \mathcal{T}} \sum_{f \in \mathcal{F}} U(x_f[t]), \qquad \mathcal{T} = \{T_{stable}, T_{stable} + 0.1, ..., T\}, \tag{5.5}$$

where T_{stable} is the point where the flow rates appear to begin to stabilize (determined empirically) and T is the simulation time.

- Optimum sum of utility: This is the optimal sum of utility as seen in (4.12), given that C equals the average throughput, $TP_{avg}(T_{stable}, T)$, for that simulation.

In the 4-flow and 8-flow scenario the weights for the flows are $\boldsymbol{\beta}_f = [1, 2, 3, 4]$ and $\boldsymbol{\beta}_f = [1, 2, 3, 4, 5, 6, 7, 8]$ respectively. Figure 5.2 shows the normalized flow rates with respect to time for one simulation. The flow rates are normalized with respect to $\min_f(x^\star_f)$, given that $x^\star_f$ represents the optimal flow rate for flow f according to (4.10), where C in this case is the average throughput in the simulation. For example, in the 4-flow 802.11 case, the average throughput is 108.59 pkts/s. Therefore, $\min_f(x^\star_f) =$ 10.86 pkts/s.

In addition to Table 5.1, the parameters used in these simulations are given in Table 5.2. The scenario statistics can be found in Tables 5.3 and 5.4. In the table, we show the average throughput, average sum of utility, optimal sum of utility, and the sum of utility if the flows were all uniform. The optimal sum term is calculated using (4.12) where C is the average throughput in this case. The uniform sum term

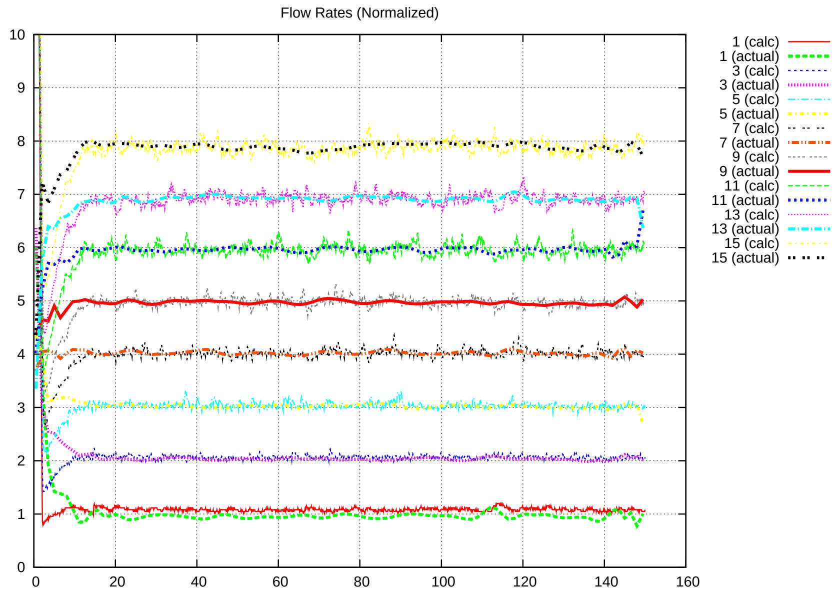

Figure 5.2: The flow rates for a normalized flow. $\Delta_{bp} = 1.0$, Scheme 1.

Table 5.2: NS2 scenario properties for the LAN simulations.

Property	Value	Unit
K	100	-
α	0.1	-
σ	10	-
CW_{umin}	31	-
CW_{umax}	511	-

Table 5.3: Statistics from the circle scenario simulations. The weights for the 4- and 8-flow cases with $\boldsymbol{\beta}_f = [1, 2, 3, 4]$ and $\boldsymbol{\beta}_f = [1, 2, 3, 4, 5, 6, 7, 8]$, respectively. Throughput is given in pkts/s.

		Avg. Throughput		Avg. Sum of Util		Optimal SoU		Uniform SoU	
		4-flow	8-flow	4-flow	8-flow	4-flow	8-flow	4-flow	8-flow
802.11		108.59	120.46	32.92	96.87	34.077	102.76		
Δ_{bp}	Scheme								
0.1	1	102.60	106.89	33.43	96.10	33.51	98.46	32.45	93.32
0.5	1	105.94	108.60	33.74	97.76	33.83	99.03	32.77	93.89
1.0	1	106.44	109.67	33.79	98.22	33.88	99.38	32.81	94.25
2.0	1	106.71	110.44	33.82	98.43	33.90	99.63	32.84	94.50
5.0	1	106.83	111.15	33.81	98.57	33.91	99.86	32.85	94.73
0.1	2	96.82	100.50	32.77	94.49	32.93	96.24	31.86	91.10
0.5	2	102.34	105.80	33.39	97.35	33.48	98.09	32.42	92.95
1.0	2	102.85	107.38	33.41	97.96	33.53	98.62	32.47	93.49
2.0	2	103.27	107.99	33.48	98.24	33.57	98.83	32.51	93.69
5.0	2	103.28	108.66	33.47	98.47	33.58	99.05	32.51	93.91

Table 5.4: Statistics from the circle scenario simulations. The weights for the 4- and 8-flow cases with $\boldsymbol{\beta}_f = [1, 10, 100, 1000]$ and $\boldsymbol{\beta}_f = [1, 3, 10, 32, 100, 316, 1000, 3162]$, respectively. Throughput is given in pkts/s.

		Avg. Throughput		Avg. Sum of Util		Optimal SoU		Uniform SoU	
		4-flow	8-flow	4-flow	8-flow	4-flow	8-flow	4-flow	8-flow
802.11		108.59	120.46	3667.70	15744.83	4807.70	17939.79		
Δ_{bp}	Scheme								
0.1	1	105.76	104.85	4760.17	17091.60	4778.40	17298.04	3638.40	15103.08
0.5	1	107.95	108.27	4742.41	17073.40	4801.20	17446.33	3661.20	15251.37
1.0	1	108.37	109.14	4731.73	16982.40	4805.50	17483.46	3665.50	15288.50
2.0	1	108.58	109.61	4728.19	16936.00	4807.60	17503.33	3667.60	15308.37
5.0	1	108.72	109.82	4724.56	16900.20	4809.10	17512.18	3669.10	15317.22
0.1	2	102.30	101.44	4728.66	16761.60	4741.50	17145.15	3601.50	14950.19
0.5	2	105.12	105.86	4709.41	16964.00	4771.70	17342.37	3631.60	15147.41
1.0	2	105.58	106.79	4698.60	16858.70	4776.50	17382.81	3636.50	15187.85
2.0	2	105.84	107.26	4692.75	16801.90	4779.20	17403.12	3639.20	15208.16
5.0	2	105.97	107.52	4689.50	16766.30	4780.60	17414.31	3640.60	15219.35

is the sum of the utilities if all flows were equal. A graphical representation of the data in Tables 5.3 and 5.4 can be seen in Figure 5.3.

Analysis of data

First, let us discuss the overall average throughput. As expected, due to the addition of the backpressure broadcast packets, the overall throughput in all but one simulation was less than the 802.11 baseline of 108.59 pkts/s and 120.46 pkts/s in the 4- and 8-flow cases, respectively. Also, the throughput increased as Δ_{bp} increased. This also is expected since there is now less overhead.

When comparing schemes 1 and 2 in all the trials, scheme 1 achieves higher throughput for every Δ_{bp} value, respectively. In scheme 1, the backoff value, bv, is chosen randomly from the uniform distribution $[0, CW_{min}]$, where CW_{min} is calculated according to (4.13). But, in scheme 2, the backoff value is chosen from an interval $[CW_{avg} - \sigma, CW_{avg} + \sigma]$, as seen in (4.15) and (4.16). Thus, in schemes 1 and 2 the average backoff value, ignoring the effects of exponential backoff, would be $CW_{min}/2$ and CW_{avg}, respectively. Since CW_{min} and CW_{avg} are equal according to (4.13) and (4.14), scheme 1 results in the nodes having a backoff value which is, on

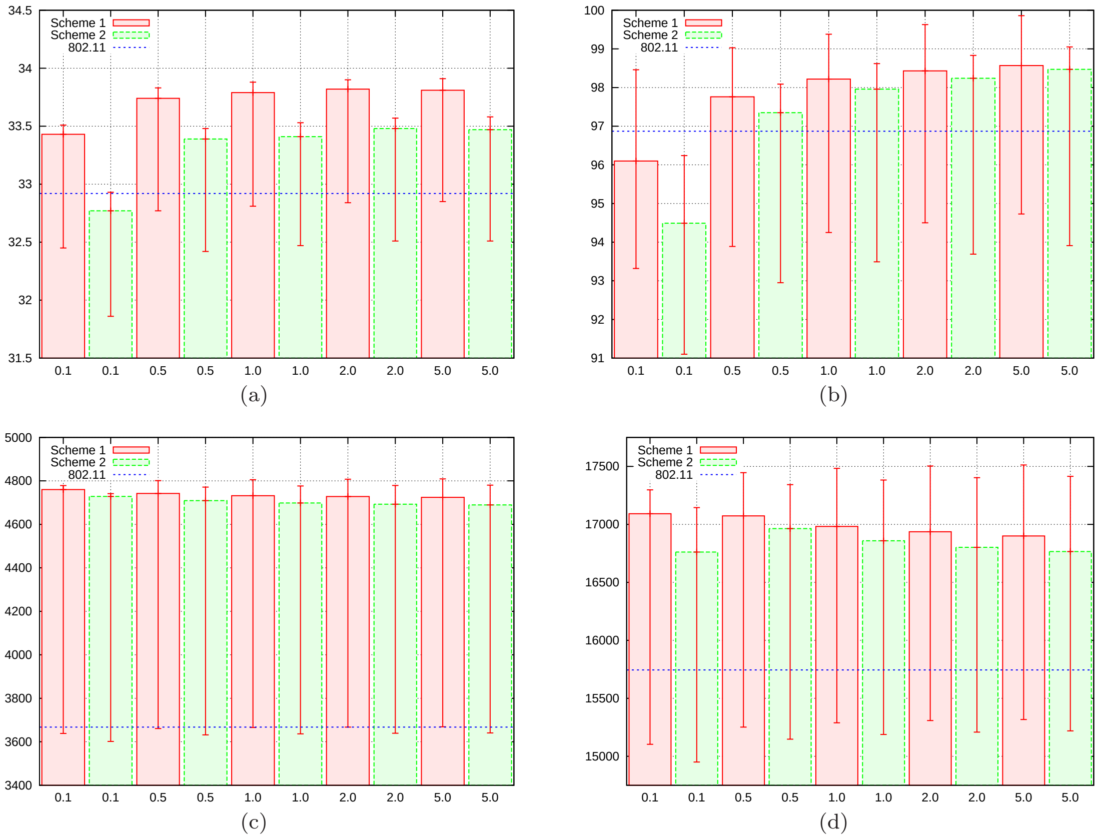

Figure 5.3: Statistics for the (a) (4-flow, $\boldsymbol{\beta}_f = [1, 2, 3, 4]$), (b) (8-flow, $\boldsymbol{\beta}_f = [1, 2, 3, 4, 5, 6, 7, 8]$), (c) (4-flow, $\boldsymbol{\beta}_f = [1, 10, 100, 1000]$), and (d) (8-flow, $\boldsymbol{\beta}_f = [1, 3, 10, 32, 100, 316, 1000, 3162]$) circle scenario simulations. The y-axis represents the sum of the utility for all flows and the x-axis is the value for Δ_{bp} in seconds. The vertical line corresponding to each box shows the optimal sum of utility (top bar) and the sum of utility for all flows being uniform (bottom bar).

average, half that of the second scheme's backoff value. When there is a small amount of contention, a larger bv average will result in more channel idle time and, therefore, decreased throughput.

In Figure 5.3, we see the average utility ($U^{avg}_{sum}(T_{stable}, T)$) plotted as a function of the backpressure broadcast interval Δ_{bp}, with the vertical line in the middle of each bar extending from the (bottom) sum of utility if all flows were uniform (which would be the case with standard 802.11) up to the (top) maximum possible sum of utility given the achieved average throughput.

Looking at the 4- and 8-flow cases where $\boldsymbol{\beta}_f = [1, \cdots, 4]$ and $\boldsymbol{\beta}_f = [1, \cdots, 8]$, we see that $U^{avg}_{sum}(T_{stable}, T)$ is growing as Δ_{bp} grows, with one exception (4-flow case where Δ_{bp} increases from 2.0 to 5.0). This steady growth is due to the throughput increase coupled with the fact that the large broadcast interval does not hurt much in this scenario because it is a single hop route, the traffic is constant, and the scenario is symmetric. Looking at the vertical lines in the 8-flow scenario, we see that scheme 2 is higher to the maximum achievable, but scheme 1 still outperforms due to the higher throughput. That is, scheme 2 may provide a better system to correctly assign priority, but it loses in the long run due to its poor throughput when compared to scheme 1. In the 4-flow scenarios, scheme 1 with $\Delta_{bp} = 2.0$ performed the best. In the 8-flow scenarios, scheme 1 with $\Delta_{bp} = 5.0$ performed the best.

Looking at the 4- and 8-flow cases where $\boldsymbol{\beta}_f = [1, \cdots, 1000]$ and $\boldsymbol{\beta}_f = [1, \cdots, 3162]$, we see that $U_{sum}^{avg}(T_{stable}, T)$ is decreasing as Δ_{bp} increases, with one exception (8-flow case using scheme 1 where Δ_{bp} increases from 0.1 to 0.5). However, in all of these cases, the average throughput increases as Δ_{bp} increases. So, we see here that the weights make a larger difference. Because these weights are growing exponentially, it is much more important (when compared to the linear weight growth) for the flows to reach the fair rate allocation point, specifically the flows with large weights. In order to reach fair rate allocation, the nodes need up-to-date backpressure information which can be achieved by more broadcast messages (i.e., a low Δ_{bp}). Thus, in these cases, the lower Δ_{bp} values correspond to the best $U_{sum}^{avg}(T_{stable}, T)$ values. In both the 4- and 8-flow scenarios, scheme 1 with $\Delta_{bp} = 0.1$ performed the best.

In both weighting schemes, we observe that the achieved $U_{sum}^{avg}(T_{stable}, T)$ is closer to the maximum possible sum of utility in the 4-flow case than the 8-flow case. This is due to the increased contention and imperfect backpressure information. As the number of competing flows increases, the number of broadcast messages increases in the contention region and collisions happen and less accurate backpressure information is used by the scheduler, adversely effecting performance.

In Figure 5.3, we have plotted $U_{sum}^{avg}(T_{stable}, T)$ for the standard 802.11 case (i.e., no utility-based scheduler or congestion controller) shown by the blue dashed line.

In the linear weighting scheme, we see that the 802.11 case actually performs better than a few of the cases which use the utility-based scheduler and congestion controller. However, this does not happen, or even come close to happening, with the exponential weighting setup. This is because the optimal flows, $x_f^\star$, are spread out linearly for the linear weighting scheme and exponentially for the exponential weighting scheme. So, if the flows' throughputs are uniform, then it will have a worse effect on the exponential weighting scheme. One can extend this result to say that utility-based scheduling and congestion control is more effective when the weighting scheme is more diverse or spread out. Due to the limited scope of this thesis, we will limit the following two scenarios to the linear weighting scheme.

5.2.2 Multihop multiflow straight line

In the straight line simulations, we want to see how the system works when nodes are forwarding multiple flows. The 8-flow scenario layout can be seen in Figure 5.1(d), with the transmission ranges and carrier sense range shown in Figure 5.1(c). In this scenario, the forwarding nodes (n_{10}, n_9, n_8) have to forward the traffic for all flows, which all have different destinations. For example, the second flow is generated by n_{12} and is destined for n_1 via the route $n_{12} \rightarrow n_{10} \rightarrow n_9 \rightarrow n_8 \rightarrow n_1$. At the start of the simulation, all the nodes at $x = 200$ m begin transmitting packets destined for the nodes at $x = 1000$ m.

Also, unlike the circular LAN scenarios, these scenarios allow for simultaneous transmissions. The transmission and carrier sense ranges are set to 250 and 550 m, respectively. This can be seen clearly in Figure 5.1(c). This setup allows a node at $x = 200$ to transmit while a node at $x = 800$ also transmits. The following are the combinations where simultaneous transmission could occur (the numbers represent the set of nodes by their x-coordinate): [200,800], [200,1000], and [400,1000].

Analysis of data

Before we discuss any throughput or utility results, let us first discuss what is happening in Figure 5.4. The figure shows the normalized instantaneous throughput and the overall queue size for all 8 flows for one scenario, with t ranging from 0 to 50 in (a) and 0 to 500 in (b). The throughput is normalized with respect to $min_{f \in \mathcal{F}}\{x_f^\star\}$, where $x_f^\star$ is the optimal fair rate for flow f given in (3.5) and can be calculated, in this case, using (4.11). Since the weights used are $\boldsymbol{\beta}_f = [1, 2, 3, 4, 5, 6, 7, 8]$, the normalized optimal rates are also $[1, 2, 3, 4, 5, 6, 7, 8]$.

In (b), we see that the scheduler/controller is doing a pretty good job of getting the rates to their fair rate allocation point, with the exception of flows f_1, f_7, and f_8. Flow f_1 is almost twice its optimal and flows f_7 and f_8 are below their optimal points. Flows f_2-f_6 are all oscillating right around their optimal points.

Recall that the queues-per-destination and the overall queue will be abbreviated as QPFs and OQ, respectively, where the overall queue is the sum of all the QPFs at a given node.

In (a), we see the normalized throughput and the overall queue length, OQ, from $t = 0$ to $t = 50$ s. We will start from $t = 0$ and explain what is happening. At $t = 0$ the simulation begins and nodes n_{11} through n_{18} begin generating packets at a rate of 50 pkts/s, per the NS2 scenario properties given in Table 5.1. These packets are destined for nodes at $x = 1000$ and must go through the path $n_{10} \rightarrow n_9 \rightarrow n_8$. Since n_{10} is the next hop for all 8 flows, n_{10} begins to get a lot of packets and its QPFs grow quickly, as shown by the growth in the OQ. In the meantime, the QPFs at the generating nodes also grow because the channel cannot withstand a rate of 50×8 pkts/s. Between $t = 0$ and $t = 6$, due to the backpressure scheduler, n_{10}'s OQ grows linearly and n_9's OQ stays empty. This is because all of the nodes at $x = 200$ have higher backpressure values than n_{10}; therefore, n_{10} has a high backoff value and a low priority to access the channel, resulting in very few packets reaching n_9 during

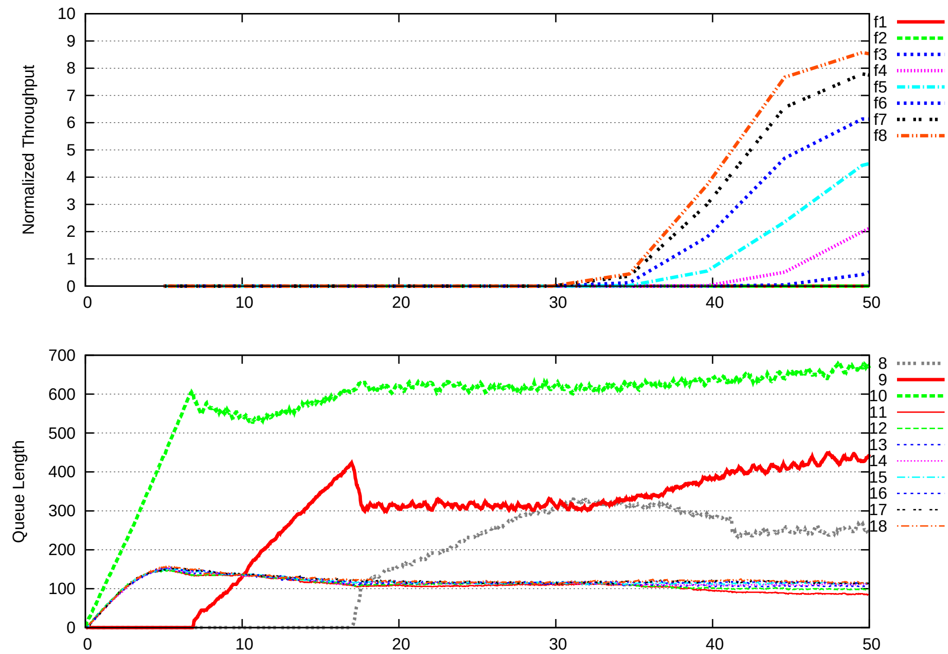

(a)

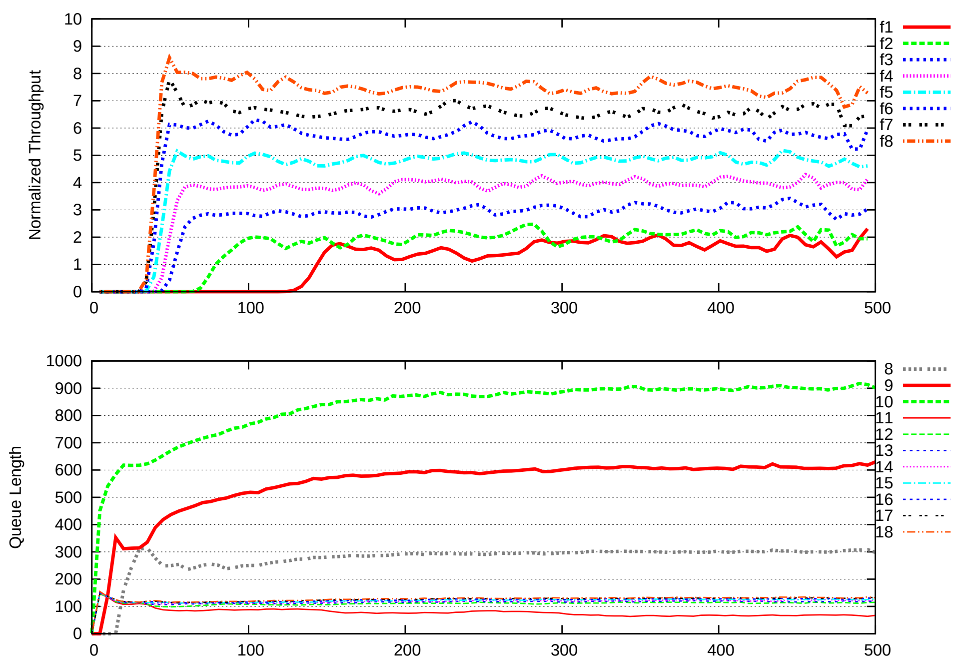

(b)

Figure 5.4: The normalized throughput for the eight flows in the straight scenario, as can be seen in Figure 5.1(d). The entire run from $t = 0$ to $t = 500$ can be seen in (b), whereas (a) is zoomed in the interval $t = [0, 50]$.

this time period. At $t = 6$, this changes and the backpressure values (one for each destination n_0-n_7) at n_{10} are now comparable to those at n_{11}-n_{18}. Thus, n_{10} begins to gain access to the channel and forwards packets to n_9. From $t = 6$ until $t = 17$, the same thing that happened at n_{10} during $t = [0, 6]$ happens at n_9. That is, the QPFs have to build up at n_9 before the backpressure values are large enough to gain a high priority to access the channel. At $t = 17$, n_9's QPFs have grown sufficiently large and can now forward packets to n_8. From $t = 17$ to $t = 31$, n_8's QPFs grow until it can forward traffic to the end destinations. At $t = 31$, we start to see packets arriving at the end destinations. However, in (b) we see that some flows do not start getting packets to their destinations until much later. Namely, f_2 and f_1 do not start getting meaningful throughput until around $t = 70$ and $t = 125$, respectively. This is due to the fact that the lower priority flows have a harder time getting packets forwarded initially due to their low priority.

In Table 5.5, we see the average throughput and the sum of utility, broken up by three time intervals, for several simulations. It is broken up into time intervals due to the large delay in forwarding of packets as can be seen in Figure 5.4. To use as comparison, the link capacity is 125 pkts/s, considering a packet size of 1000 bytes and a physical rate of 1 Mbps. Considering the interference region and taking advantage of spatial reuse, the throughput capacity is given by $\frac{125}{3}$, or 41.67 pkts/s.

In the first row we have the 802.11 baseline statistics. The 802.11 scenario was hampered by a lot of collisions which led to poor throughout. As expected, it grew a little, but was fairly uniform throughout each interval. Due to the low throughput and the uniformity in flows, the utility term was very low.

For both schemes, we varied the α and K congestion controller parameters in order to see their effect on this scenario. As stated earlier, α controls the rate of change of the flow rate. The larger α is, the faster the flow rate changes. We also tested against the two schemes and the broadcast interval, Δ_{bp}. In average throughput, scheme 1 had the maximum value in all three intervals, and also over the whole interval of [0,150],

Table 5.5: Performance of the multihop multiflow straight line simulations. Note: In calculating $U_{sum}^{avg}(\cdot,\cdot)$, if $x_f[t] = 0$ for some t, we would use $x_f[t] = 0.01$ instead due to $\ln(0) = -\infty$.

α	K	Δ_{bp}	$TP_{avg}(x,y)$ 0,50	50,100	100,150	0,150	$U_{sum}^{avg}(x,y)$ 0,50	50,100	100,150
802.11			17.76	18.8	19.7551	18.7651	26.7141	27.111	26.4652
Scheme 1									
0.1	100	0.1	22.58	25.86	29.55	25.97	31.82	43.11	50.32
0.1	100	0.5	**24.88**	27.12	30.35	**27.43**	39.17	47.44	50.24
0.1	100	1.0	24.70	28.50	28.84	27.34	**41.64**	47.44	46.69
0.1	500	0.1	14.00	24.96	27.10	21.99	-22.45	24.02	26.66
0.1	500	0.5	16.06	26.98	28.08	23.68	-32.03	21.08	27.84
0.1	500	1.0	16.36	26.62	27.61	23.50	-9.36	27.66	32.77
0.01	100	0.1	17.80	28.68	30.98	25.78	7.91	**49.57**	**52.61**
0.01	100	0.5	19.60	**29.04**	**31.10**	26.55	26.29	49.23	49.95
0.01	100	1.0	21.00	27.98	30.06	26.32	35.40	46.74	48.25
0.01	500	0.1	13.40	26.66	26.26	22.08	-16.18	28.16	32.44
0.01	500	0.5	15.26	28.06	28.45	23.89	-5.41	31.66	34.96
0.01	500	1.0	15.00	27.28	28.61	23.60	-34.44	28.06	39.13
Scheme 2									
0.1	100	0.1	8.52	25.76	28.18	20.77	-47.88	36.92	40.58
0.1	100	0.5	11.56	26.10	29.06	22.19	-40.08	41.69	47.78
0.1	100	1.0	15.66	27.08	28.69	23.78	-4.89	44.19	45.96
0.1	500	0.1	6.96	20.56	19.33	15.59	-32.78	18.55	18.99
0.1	500	0.5	13.36	23.18	21.75	19.41	-6.16	23.19	22.71
0.1	500	1.0	15.22	23.68	22.49	20.45	2.62	23.62	23.63
0.01	100	0.1	4.10	27.06	28.57	19.85	-120.36	41.60	47.13
0.01	100	0.5	15.44	27.70	*30.12*	*24.38*	7.81	45.27	*48.55*
0.01	100	1.0	*15.70*	*27.72*	29.41	24.24	*14.85*	*45.72*	46.51
0.01	500	0.1	3.92	18.90	17.88	13.54	-46.04	17.37	19.81
0.01	500	0.5	12.32	21.72	20.86	18.28	-10.31	22.33	22.91
0.01	500	1.0	13.12	22.42	22.06	19.18	-11.01	25.66	28.07

as shown by the numbers in bold. Surprisingly, in scheme 1, $\Delta_{bp} = 0.5$ provided the maximum throughput in [0,150] for all values of α and K, when compared to $\Delta_{bp} = 0.1$ and $\Delta_{bp} = 1.0$. In scheme 2, $\Delta_{bp} = 1.0$ provided the maximum in three out of the four α,K combinations. Also, notice that in both schemes, the $K = 100$ trials achieved more throughput than the $K = 500$ trials because the higher the K value is, then the higher the queue must be in order to drive Δ_{x_f} to 0. If the queue has to be larger, then it will take longer for the backpressure values at n_{10}-n_8 to level out and get the first packet of each flow to its destinations. Over the whole interval [0,150], the maximum average throughput was achieved by scheme 1 using parameters $[\alpha, K, \Delta_{bp}] = [0.1, 100, 0.5]$. As for the average of the sum utility,

U_{sum}^{avg}, scheme 1 also had the maximum value for all three intervals. With $[\alpha, K]$ being constant, $U_{sum}^{avg}(0, 50)$ increased with Δ_{bp} because more packets were making it to the destination faster due to innacurate (old) backpressure information at the intermediate nodes. With only 1 broadcast packet every second, the intermediate nodes would think that their backpressure was large enough to have priority access to the channel. However, for the other two intervals, the lower Δ_{bp} values proved better due to more accurate backpressure information. For the last two intervals, scheme 1 with parameters $[\alpha, K, \Delta_{bp}] = [0.01, 100, 0.1]$ achieved the highest U_{sum}^{avg}, with $U_{sum}^{avg}(50, 100) = 49.57$ and $U_{sum}^{avg}(100, 150) = 52.61$. These parameters will be used in the random scenarios. For that case and with $C = 30.98$, the optimal sum is 53.88 and the sum with uniform flows is 48.74.

5.2.3 Random topology

In the random topology trials, we generated scenarios with eight three-hop disjoint flows. That is, every node only forwards traffic for, at most, one node. To generate the scenarios, we first randomly placed nodes on a 1000 m x 1000 m grid. Then, for each of the eight flows, we selected a random source node and a random destination node. Using Dijktra's shortest route algorithm, a route was selected. If the route was three hops long and did not contain any nodes from any of the other flows, then it was added. Twenty of these scenarios were generated. A sample scenario is shown in Figure 5.1(f).

For the sake of brevity, we decided it was only necessary to run the random tests across one set of parameters. A good performing set of parameters from the straight-line simulations were used and can be seen in Table 5.6.

Table 5.7 shows the average throughput across all random scenarios, both for the case where the scheduler/controller was used and also for the simple 802.11 case. It is also broken down into time intervals for analyzing.

Table 5.6: NS2 scenario properties for the random simulations.

Property	Value	Unit
K	100	-
α	0.01	-
σ	10	-
CW_{umin}	31	-
CW_{umax}	511	-
Δ_{bc}	0.1	sec

Table 5.7: Overall throughput values for random scenarios.

	[0,150]	[0,25]	[25,50]	[50,75]	[75,100]	[100,125]	[125,150]
802.11	31.09	30.17	31.47	31.39	31.38	31.30	30.83
Scheme 1	25.80	9.09	27.73	28.73	29.57	29.88	30.01
Scheme 2	23.43	4.69	22.12	26.64	28.74	29.11	29.53

Analysis of data

In Table 5.7, we see the throughput for both schemes and the 802.11 case averaged over 20 random scenarios. Overall, we see that scheme 1 has a higher throughput at 25.80 pkts/s, compared to 23.43 pkts/s for scheme 2. This is more than 5 pkts/s less than the 802.11 case, but this can be explained. Similar to the multihop multiflow straight line simulations, the average throughput suffers a lot at the beginning of the trial because the QPFs at all nodes are zero. The [0,25] interval throughput is very low at 9.09 and 4.69 for schemes 1 and 2, but then more than doubles for the [25,50] interval. Looking at Figures 5.5(a) and 5.5(b), one can see that the throughput increases significantly. In the final interval [125,150], the average throughput is only 0.82 and 1.30 pkts/s less than the 802.11 case, for schemes 1 and 2, respectively. The average throughput for scheme 2 is less because, as mentioned previously, the average backoff value is greater than that of scheme 1 and there is more idle channel time.

For the average sum of utility printed in Table 5.8, we see that standard 802.11 is the greatest for the first two intervals. This is once again due to the low throughput for these intervals. In the next four intervals, scheme 1 has the greatest $U^{avg}_{sum}(\cdot,\cdot)$, with the sum growing with time. We can see the fair rate allocation point being

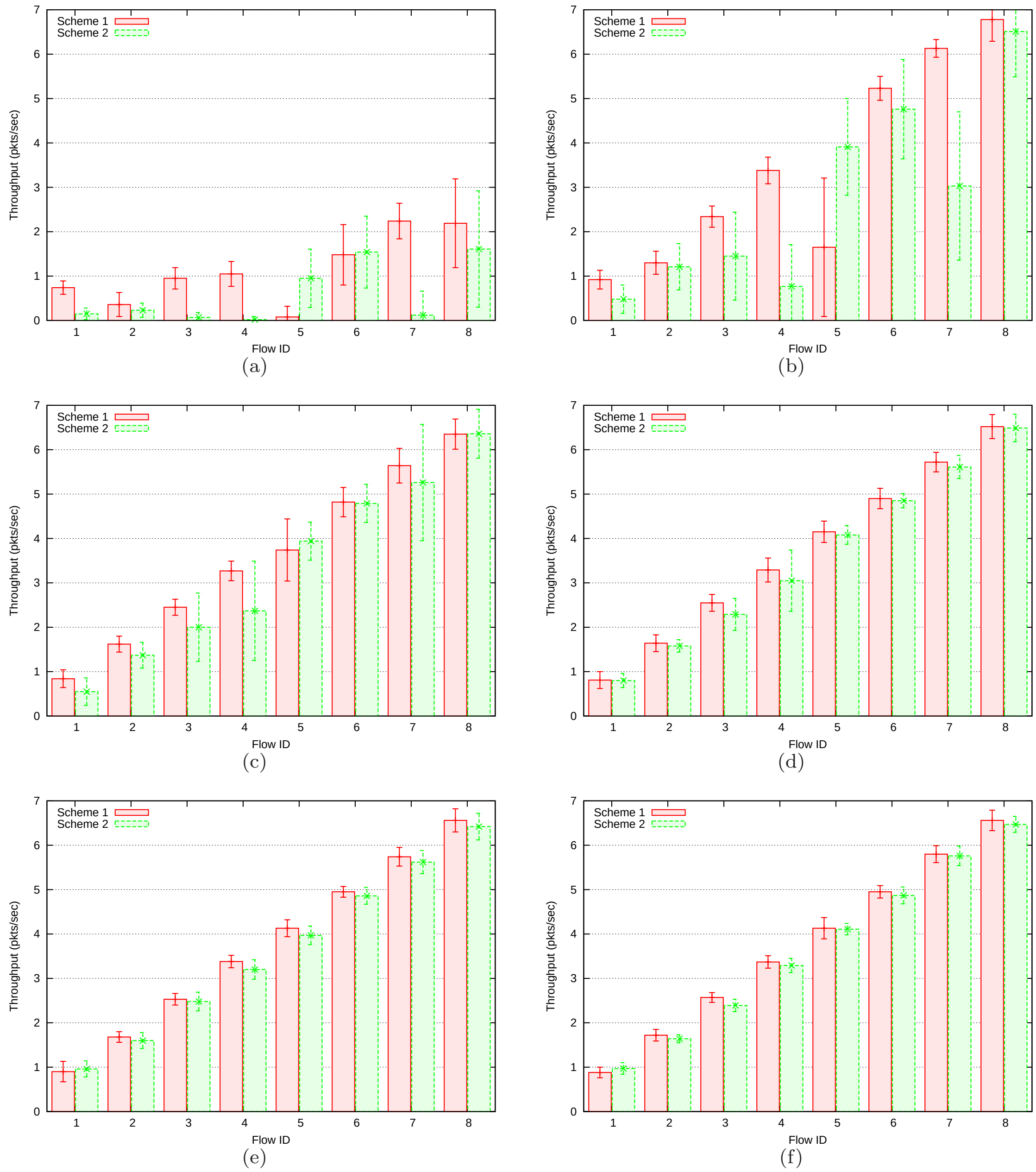

Figure 5.5: Throughput of the flows in the random scenarios. The throughput was averaged across all 20 runs and the error bar shows the standard deviation of each flow. The plots are for time intervals (a) [0:25], (b) [25:50], (c) [50:75], (d) [75,100], (e) [100,125], and (f) [125,150] seconds.

Table 5.8: Sum of utility values for random scenarios.

	[0,25]	[25,50]	[50,75]	[75,100]	[100,125]	[125,150]
802.11	**48.23**	**48.59**	48.27	48.40	48.36	47.83
std_dev	1.16	0.88	1.33	1.31	1.16	1.07
Scheme 1	-27.94	35.76	**48.92**	**51.06**	**51.59**	**51.73**
std_dev	20.51	10.96	4.50	2.02	0.44	0.40
Scheme 2	-101.09	6.66	38.58	48.74	50.38	51.16
std_dev	25.60	25.05	15.58	5.22	2.93	0.40

reached visually by looking at Figure 5.5, and noticing that with each increase in interval, the flow rates approach a fair point and the standard deviation decreases. Also, in Table 5.8, we see that the standard deviation is decreasing as t increases, which tells us that both schemes are stabilizing.

5.3 Summary of Simulations

In the LAN simulations, we saw that the system, despite adding some extra overhead into the network, could outperform standard 802.11 in the sum of the utilities of the flows. We also saw that neither scheme could reach the fair rate allocation point exactly given the achieved throughput, but both performed much better than the case where the flow rates were all equal.

In the multihop multiflow straight line simulations, we saw that forwarding nodes could adequately handle multiple flows with multiple destinations. In doing so, the packets were delayed due to necessary queue buildup and the throughput suffered initially. After the initial delay, the sum of utility clearly outperformed that of 802.11.

In the random scenario analysis, we saw that the fair rate allocation point was being approached as t increased, despite the random nature of the scenarios. The average throughput suffered initially, as in the straight line experiments, but in the later intervals approached that of 802.11.

Overall, scheme 1 provided a higher sum of utility than the second scheme. However, more work should be done to see the effect of lowering CW_{umin} in order to lower the average backoff value for the second scheme. As far as the backpressure broadcast, ten per second ($\Delta_{bp} = 0.1$) seemed to work the best in multihop situations, whereas one every two seconds seemed adequate for the LAN one-hop scenario.

CHAPTER 6

CONCLUSIONS AND FUTURE WORK

In this thesis, we propose a distributed backpressure-based congestion controller and scheduler system, based upon the controller-scheduler described in [1]. This system allows for flows within a wireless network to be assigned a weighted utility that is a function of the flow rate. The goal of the system is to maximize the sum of all of the utilities of all the flows in the network, as seen in (3.5).

In our simulations, we showed that while the flow rates did not converge to the optimal solution, they did converge very closely at times and almost always performed better than standard 802.11. Our simulations highlighted the performance of this distributed system in three topologies: a simple LAN, a fixed multihop scenario, and a random multihop scenario. We also compared two different schemes for the backpressure-based scheduler.

We believe that, although a lot was learned through the work performed in this thesis, there is still more work that needs to be done. Thus, we would like to propose some future work. The following list highlights some of the areas/ideas that we would like to pursue to extend this distributed controller-scheduler in attempt to establish a solid framework:

- Physical layer rate control: Instead of controlling the flow rate at the MAC layer, one could harness the power of the physical layer rate control.
- Move the broadcast packets down to the MAC layer: Currently, mainly due to simulation ease, the broadcast packets come from the application layer even though they should be generated by the MAC layer. In future simulations, we

should move all of the scheduler components down to the MAC layer.

- Evaluate non-802.11 based system: In our simulations, we took the standard 802.11 MAC and physical layer and modified it to incorporate our scheduler and controller. It would be valuable to look at a clean slate approach and not restrict oneself to the confines of the 802.11 standard.

REFERENCES

[1] A. Eryilmaz and R. Srikant, "Joint congestion control, routing, and MAC for stability and fairness in wireless networks," *IEEE Journal on Selected Areas in Communications*, vol. 24, no. 8, pp. 1514–1524, 2006.

[2] The network simulator—ns-2. [Online]. Available: http://www.isi.edu/nsnam/ns/.

[3] M. S. Gast, *802.11 Wireless Networks: The Definitive Guide*, M. Loukides, Ed. Sebastopol, CA: O'Reilly & Associates, Inc., 2002.

[4] LAN/MAN Standards Committee of the IEEE Computer Society. ANSI/IEEE Std 802.11, 1999 Edition (R2003). [Online]. Available: http://standards.ieee.org/getieee802/802.11.html.

[5] J. Deng and R.-S. Chang, "A priority scheme for IEEE 802.11 DCF access method," *IEICE Transactions on Communication*, vol. E82-B, no. 1, pp. 96–102, 1999.

[6] Y. Xiao, "A simple and effective priority scheme for IEEE 802.11," *IEEE Communication Letters*, vol. 7, no. 2, pp. 70–72, 2003.

[7] N. Vaidya, A. Dugar, S. Gupta, and P. Bahl, "Distributed fair scheduling in a wireless LAN," *IEEE Transactions on Mobile Computing*, vol. 4, no. 6, pp. 616–629, 2005.

[8] L. Tassiulas and A. Ephremides, "Stability properties of constrained queueing systems and scheduling policies for maximum throughput in multihop radio networks," *IEEE Transactions on Automatic Control*, vol. 37, no. 12, pp. 1936–1948, 1992.

[9] H. Yaiche, R. R. Mazumdar, and C. Rosenberg, "A game-theoretic framework for bandwidth allocation and pricing in broadband networks," *IEEE/ACM Transactions on Networking*, vol. 8, no. 5, pp. 667–678, 2000.

[10] S. Kunniyur and R. Srikant, "A time-scale decomposition approach to adaptive ECN marking," *IEEE Transactions on Automatic Control*, vol. 47, no. 6, pp. 882–894, 2002.

[11] T. Alpcan and T. Başar, "A utility-based congestion control scheme for internet-style networks with delay," in *Proceedings of IEEE INFOCOM*, San Francisco, CA, March 2003, pp. 2039–2048.

[12] F. P. Kelly, A. Maulloo, and D. Tan, "Rate control in communication networks: Shadow prices, proportional fairness and stability," *Journal of the Operational Research Society*, vol. 49, no. 3, pp. 237–252, 1998.

[13] S. H. Low and D. E. Lapsley, "Optimization flow control, I: Basic algorithm and convergence," *IEEE/ACM Transactions on Networking*, vol. 7, no. 6, pp. 861–874, 1999.

[14] J. T. Wen and M. Arcak, "A unifying passivity framework for network flow control," *IEEE Transactions on Automatic Control*, vol. 49, no. 2, pp. 162–174, 2004.

[15] A. Eryilmaz and R. Srikant, "Fair resource allocation in wireless networks using queue-length based scheduling and congestion control," in *Proceedings of IEEE INFOCOM*, Miami, FL, March 2005, pp. 1794–1803.

[16] L. Chen, S. H. Low, and J. C. Doyle, "Joint congestion control and media access control design for wireless ad hoc networks," in *Proceedings of IEEE INFOCOM*, Miami, FL, March 2005, pp. 2212–2222.

[17] X. Lin and N. Shroff, "The impact of imperfect scheduling on cross-layer rate control in multihop wireless networks," in *Proceedings of IEEE INFOCOM*, Miami, FL, March 2005, pp. 1804–1814.

[18] Y. Yi and S. Shakkottai, "Hop-by-hop congestion control over a wireless multi-hop network," in *Proceedings of IEEE INFOCOM*, Hong Kong, March 2004, pp. 2548–2558.

[19] M. Chiang, "To layer or not to layer: Balancing transport and physical layers in wireless multihop networks," in *Proceedings of IEEE INFOCOM*, Hong Kong, March 2004, pp. 2525–2536.

[20] L. Chen, S. H. Low, M. Chiang, and J. C. Doyle, "Cross-layer congestion control, routing and scheduling design in ad hoc wireless networks," in *Proceedings of IEEE INFOCOM*, Barcelona, Spain, April 2006, pp. 1–13.

[21] X. Lin and N. Shroff, "Joint rate control and scheduling in multihop wireless networks," in *Proceedings of the IEEE Conference on Decision and Control*, Paradise Island, Bahamas, Dec. 2004, pp. 1484–1489.

[22] A. Stolyar, "Maximizing queueing network utility subject to stability: Greedy primal-dual algorithm," *Queuing Systems*, vol. 50, no. 4, pp. 401–457, 2005.

[23] M. J. Neely, E. Modiano, and C. Li, "Fairness and optimal stochastic control for heterogeneous networks," in *Proceedings of IEEE INFOCOM*, Miami, FL, March 2005, pp. 1723–1734.

[24] L. Tassiulas and S. Sarkar, "Maxmin fair scheduling in wireless networks," in *Proceedings of IEEE INFOCOM*, New York, NY, June 2002, pp. 763–772.

[25] X. Wu and R. Srikant, "Regulated maximal matching: A distributed scheduling algorithm for multi-hop wireless networks with node-exclusive spectrum sharing," in *Proceedings of the IEEE Conference on Decision and Control*, Seville, Spain, Dec. 2005, pp. 5342–5347.

[26] L. Bui, A. Eryilmaz, R. Srikant, and X. Wu, "Joint asynchronous congestion control and distributed scheduling for wireless networks," in *Proceedings of IEEE INFOCOM*, Barcelona, Spain, April 2006, pp. 1–12.

[27] P. Chaporkar, K. Kar, and S. Sarkar, "Throughput guarantees through maximal scheduling in wireless networks," in *Proceedings of the Allerton Conference on Communication, Control, and Computing*, Urbana, IL, Sept. 2005, pp. 1557–1567.

[28] X. Wu and R. Srikant, "Scheduling efficiency of distributed greedy scheduling algorithms in wireless networks," in *Proceedings of IEEE INFOCOM*, Barcelona, Spain, April 2006, pp. 1–12.

[29] J. Mo and J. Walrand, "Fair end-to-end window-based congestion control," *IEEE/ACM Transactions on Networking*, vol. 8, no. 5, pp. 556–567, 2000.

[30] K. Fall and K. Varadhan, "The ns manual," 2007. [Online]. Available: http://www.isi.edu/nsnam/ns/ns-documentation.html.

[31] "NS-MIRACLE: Multi-interface cross-layer extension library for the network simulator," 2007. [Online]. Available: http://www.dei.unipd.it/wdyn/?IDsezione=3966.

[32] T. S. Rappaport, *Wireless Communications: Principles and Practice.* Upper Saddle River, NJ: Prentice Hall PTR, 2002.